

# Akt phosphorylates the Y-box binding protein 1 at Ser102 located in the cold shock domain and affects the anchorage-independent growth of breast cancer cells

Brent W Sutherland<sup>1</sup>, Jill Kucab<sup>2</sup>, Joyce Wu<sup>2</sup>, Cathy Lee<sup>2</sup>, Maggie CU Cheang<sup>3</sup>, Erika Yorida<sup>3</sup>, Dmitry Turbin<sup>3</sup>, Shoukat Dedhar<sup>4</sup>, Colleen Nelson<sup>5</sup>, Michael Pollak<sup>6</sup>, H Leighton Grimes<sup>7</sup>, Kathy Miller<sup>8</sup>, Sunil Badve<sup>9</sup>, David Huntsman<sup>3</sup>, C Blake-Gilks<sup>3</sup>, Min Chen<sup>10,11</sup>, Catherine J Pallen<sup>11</sup> and Sandra E Dunn<sup>\*,2</sup>

<sup>1</sup>Clinical Research Division, Fred Hutchinson Cancer Center, Seattle, WA, USA; <sup>2</sup>Laboratory for Oncogenomic Research, Department of Pediatrics, British Columbia Research Institute for Children's and Women's Health, Vancouver, British Columbia, Canada; <sup>3</sup>Genetic Pathology Evaluation Center, Vancouver Hospital and Health Sciences Center and BC Cancer Agency, Vancouver, British Columbia, Canada; <sup>4</sup>British Columbia Cancer Agency, Vancouver, British Columbia, Canada; <sup>5</sup>Prostate Center at Vancouver General Hospital, Jack Bell Research Laboratories, Vancouver, British Columbia, Canada; <sup>6</sup>Division of Experimental Medicine, Department of Medicine and Department of Oncology, McGill University, Montreal, Quebec, Canada; <sup>7</sup>Institute for Cellular Therapeutics, Louisville, KY, USA; <sup>8</sup>Department of Medicine, Indiana University, Bloomington, IN, USA; <sup>9</sup>Department of Pathology, Indiana University, Bloomington, IN, USA; <sup>10</sup>Institute of Molecular and Cell Biology, Singapore; <sup>11</sup>Cell Phosphosignaling Laboratory, Department of Pediatrics, British Columbia Research Institute for Children's and Women's Health, Vancouver, British Columbia, Canada

**Akt/PKB is a serine/threonine kinase that promotes tumor cell growth by phosphorylating transcription factors and cell cycle proteins. There is particular interest in finding tumor-specific substrates for Akt to understand how this protein functions in cancer and to provide new avenues for therapeutic targeting. Our laboratory sought to identify novel Akt substrates that are expressed in breast cancer. In this study, we determined that activated Akt is positively correlated with the protein expression of the transcription/translation factor Y-box binding protein-1 (YB-1) in primary breast cancer by screening tumor tissue microarrays. We therefore questioned whether Akt and YB-1 might be functionally linked. Herein, we illustrate that activated Akt binds to and phosphorylates the YB-1 cold shock domain at Ser102. We then addressed the functional significance of disrupting Ser102 by mutating it to Ala102. Following the stable expression of Flag:YB-1 and Flag:YB-1 (Ala102) in MCF-7 cells, we observed that disruption of the Akt phosphorylation site on YB-1 suppressed tumor cell growth in soft agar and in monolayer. This correlated with an inhibition of nuclear translocation by the YB-1(Ala102) mutant. In conclusion, YB-1 is a new Akt substrate and disruption of this specific site inhibits tumor cell growth.**

**Keywords:** breast cancer; Akt; YB-1; phosphorylation; cold shock domain; signal transduction

## Introduction

Akt (or protein kinase B, PKB) is a family of serine/threonine kinases that inhibit apoptosis, stimulate angiogenesis, and promote tumor formation (reviewed in Nicholson and Anderson, 2002). There are presently three known isoforms, Akt-1, Akt-2 and Akt-3, that have all been linked to the development of cancer (Hill and Hemmings, 2002). Several tyrosine kinase receptors activate Akt including the insulin-like growth factor-1 receptor (IGF-1R) (Dunn *et al.*, 2001). The IGF-1 ligand binds to its receptor, IGF-1R, and triggers signaling events including activation of the phosphatidylinositol-3 kinase (PI3K) pathway thereby releasing lipid second messengers to recruit Akt to the plasma membrane. Akt is then phosphorylated at the Thr308 site by phosphatidylinositol-dependent kinase-1 (PDK-1) with subsequent phosphorylation of Ser473 either by autophosphorylation (Brazil and Hemmings, 2001), interaction with integrin-linked kinase (ILK) (Persad *et al.*, 2001), or through DNA-PK (Feng *et al.*, 2004). Once Akt is activated, it binds to and phosphorylates substrates with RxRxxS/T or RxxT motifs including transcription factors and cell cycle proteins such as forkhead L1 (Brunet *et al.*, 1999), AFX (Kops *et al.*, 1999), p21 (Zhou *et al.*, 2001), and p27 (Shin *et al.*, 2002). The net effect of substrate phosphorylation is an initial shift in subcellular trafficking followed by an increase in cell proliferation and

suppression of cell cycle arrest. Hence, Akt phosphorylates a wide range of proteins resulting in a change in their function.

The Y-box binding protein-1 (YB-1) is a protein that has multiple functions including regulation of gene expression and progression of the cell cycle. YB-1 is highly expressed in cancers of the breast (Bargou *et al.*, 1997) and the prostate (Gimenez-Bonafe *et al.*, 2004). To explore how YB-1 may alter the cancer phenotype, Royer and co-workers (Bargou *et al.*, 1997) expressed it in pre-neoplastic breast epithelial cells, which caused them to be resistant to doxorubicin along with a concomitant increase in the expression of multidrug-resistant gene-1 (MDR). They also concluded that YB-1 was not expressed in normal breast tissue but was highly expressed in tumors (Bargou *et al.*, 1997), a finding that was subsequently confirmed (Rubinstein *et al.*, 2002). Therefore, YB-1 is preferentially expressed in breast tumors relative to normal tissue and may play a role in drug resistance. Although more recently, YB-1 is reported to stimulate proliferation of pre-neoplastic breast cancer cells by inducing cyclin A and B mRNA (Jurchott *et al.*, 2003), this is certainly consistent with the growth-enhancing potential of YB-1 in other cancers. For example, YB-1 positively correlates with the expression of the proliferating cell nuclear antigen and a high proliferative index in colorectal tumors (Shibao *et al.*, 1999). Direct evidence for the role of YB-1 in cell proliferation comes from gene knock-down experiments where one of the alleles was deleted. The hemizygous disruption of YB-1 in the chicken lymphocytic cell line, DT40, remarkably suppresses cell growth (Swamynathan *et al.*, 2002). After 3 days in culture, loss of YB-1 suppressed cell growth by >70%. The loss of YB-1 expression led to disruption of the cell cycle at the G2/M transition (Swamynathan *et al.*, 2002). The growth potential of YB-1 is also reported in chickens undergoing liver regeneration (Grant and Deeley, 1993). Several studies therefore indicate that YB-1 positively regulates cell growth. However, these studies are in contrast to a report indicating that YB-1 has growth suppressive effects in chicken embryo fibroblasts (Bader *et al.*, 2003). Thus, the dependency for YB-1 to promote proliferation may be cell type specific. More central to our interest is whether or not tumor cells depend on YB-1 for growth and survival. Based upon one report, it appears that tumor cells are dependent on YB-1 because melanoma, adenocarcinoma, hepatoma, fibrosarcoma, and colon cancer cells die when its expression is knocked out with antisense RNA (Lasham *et al.*, 2003). The underlying mechanisms governing YB-1-mediated growth are also not understood. We anticipate that YB-1 is part of an undefined signal transduction network.

YB-1 translocates between the cytoplasm and the nucleus in an as yet undefined manner. Nuclear YB-1 is associated with drug resistance and the expression of MDR in breast cancer (Bargou *et al.*, 1997), synovial sarcomas (Oda *et al.*, 2003), and osteosarcomas (Oda *et al.*, 1998). Because of its role in drug resistance, patients who have tumors with YB-1 may be less responsive to therapy. This becomes evident in ovarian

cancer where nuclear YB-1 is found in cisplatin-resistant cell lines. Comparisons were made to cisplatin-sensitive cell lines where YB-1 was not located in the nucleus (Yahata *et al.*, 2002). In paired surgical specimens of ovarian cancer, YB-1 was also notably expressed in the tumors that failed treatment with cisplatin (Yahata *et al.*, 2002). Likewise, the expression of nuclear YB-1 relates to increased rates of relapse for women with ovarian cancer (Yahata *et al.*, 2002). Finally, the disease-free survival is significantly worse for breast (Janz *et al.*, 2002) and ovarian (Kamura *et al.*, 1999) cancer patients who have had tumors expressing nuclear YB-1. It is presently unclear what signaling pathway triggers YB-1 to move into the nucleus of cancer cells. Stimuli such as UV irradiation (Koike *et al.*, 1997) and chemotherapeutic agents (Okamoto *et al.*, 2000) cause YB-1 to traffic into the nucleus. Albeit these events lead to the nuclear translocation of YB-1, there must be other signals that impart this effect, particularly in light of a report indicating that YB-1 is in the nucleus of breast tumors that have not previously been treated with chemotherapy or irradiation (Bargou *et al.*, 1997). Previously untreated osteosarcomas also express YB-1 in the nuclear compartment (Oda *et al.*, 1998). Therefore, it is unclear what causes YB-1 to traffic into the nucleus in tumors. Extracellular signals are a possibility. For example, thrombin stimulates the translocation of YB-1 into the nucleus and regulates the expression of the vascular mitogen platelet-derived growth factor (PDGF) in endothelial cells (Stenina *et al.*, 2000). Interestingly, this pathway is blocked using inhibitors of protein tyrosine phosphatases (Stenina *et al.*, 2000). It has also been suggested that interferon activates the Janus kinase and casein kinase II pathways resulting in the translocation of YB-1 into the nucleus (Higashi *et al.*, 2003). These data indicate that there are signal transduction pathways that alter the subcellular localization of YB-1 and as such direct its function.

Given that the PI3K/Akt pathway is a key regulator of cancer cell proliferation, there is interest in taking therapeutic approaches to targeting this signaling network. We recently screened tumor tissue microarrays (TMAs) to determine how often phosphorylated Akt (P-Akt) was present in breast cancer and found that it was moderately to highly expressed in 58% (225/390 cases) of tumors (Kucab *et al.*, Celecoxib analogues disrupt Akt signaling which is commonly activated in primary breast tumors, submitted). In the study described here, we sought to understand how Akt might be functioning in breast cancer by profiling the protein expression of 30 proteins using TMAs. We had also hoped to find novel substrates that might be coordinately regulated, which would provide more insight into how Akt functions in a tumor-specific manner. From this screen, we found that P-Akt was coordinately expressed with YB-1 in primary tumors. Thus, we elected to focus on the potential relationship between P-Akt and YB-1 for subsequent studies. We determined that P-Akt binds to YB-1 and phosphorylates it on the cold shock domain (CSD). Furthermore, we mapped the phosphorylation site to Ser102 and show that disruption of this site alters

anchorage-independent growth. Serum-induced cell growth in monolayer was also dependent upon YB-1(Ser102). Finally, we determined that in the presence of serum there was less YB-1 in the nucleus when the Ser102 site was mutated to Ala102. Thus, we have provided the first evidence that YB-1 is a novel substrate for Akt.

## Results and discussion

### *P-Akt and YB-1 are coordinately expressed in primary breast tumors*

Breast cancer TMAs were immunostained for the expression of P-Akt. We then queried a database that contained the expression profiles of 30 other proteins. After integrating > 12 000 data points, we determined that the expression of P-Akt was significantly correlated with the expression of six other proteins, using univariate analysis (Supplementary Table 1). Of the six proteins, three were tyrosine kinase receptors (IGF-1R ( $P=0.000$ ), HER-2 ( $P=0.012$ ), and EphA2 ( $P=0.001$ )). We also discovered that the expression of ILK correlated with P-Akt expression ( $P=0.004$ ). Lastly, the expression of two transcription factors, growth factor independence-1 (GFI-1) ( $P=0.016$ ) and YB-1 ( $P=0.004$ ), was positively correlated with expression of P-Akt. Since Akt is known to phosphorylate other transcription and translation factors, it was conceivable that it had a similar effect on YB-1. They were indeed coordinately expressed in both the cytoplasm and the nucleus (Figure 1a). Therefore, this initial screen led us to hypothesize that P-Akt and YB-1 may be functionally linked. Given these data, we proposed that YB-1 may be a signaling intermediate downstream of the growth factor/Akt pathway (Figure 1b). This schematic provides a cellular context for the signaling molecules that were coexpressed with P-Akt. Relationships that have previously been established using cell culture models are represented (solid line) as well as those that are theoretical (broken line).

### *P-Akt binds to and phosphorylates YB-1*

To examine the possibility that YB-1 may be involved the IGF-1R/Akt signaling pathway, we turned to using well-established cell-based models of breast cancer. We selected the MDA-MB-231 cells because we previously reported that IGF-1 activates Akt in these cells (Dunn *et al.*, 2001). The MDA-MB-231 breast cancer cells were stimulated with IGF-1 for 30 min and then Akt was immunoprecipitated from the cytoplasmic fraction with the 5G3 antibody and blotted for YB-1. Akt and YB-1 co-immunoprecipitated from IGF-1-stimulated cells (Figure 2a, lane 2) more so than without stimulation (Figure 2a, lane 1). This correlated with high levels of P-Akt following IGF-1 stimulation (Figure 2a, lane 2, middle panel). From these data, we suspected that Akt had to be activated in order to bind to YB-1. We were fairly confident that the binding was specific because

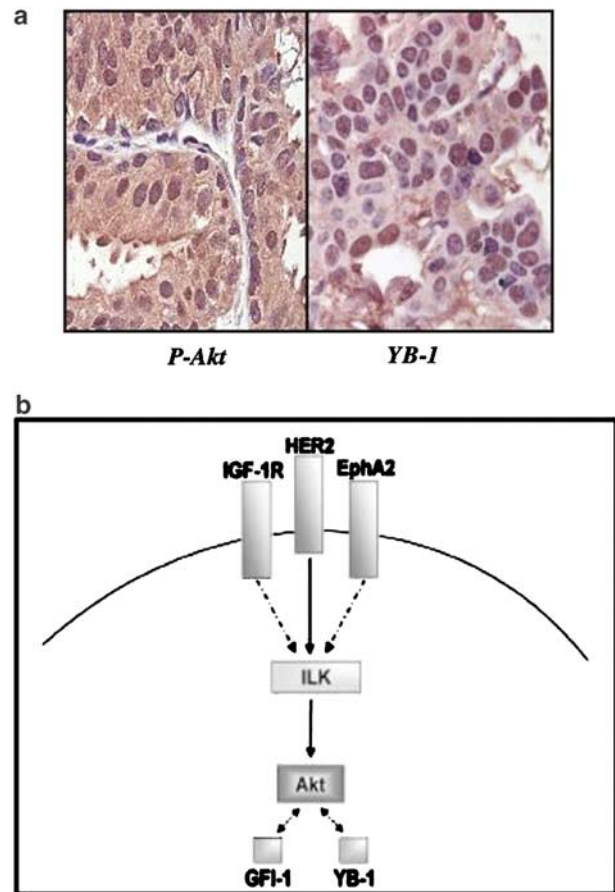


**Figure 1** P-Akt signaling network in breast cancer based on expression profiling TMAs. (a) Examples of P-Akt and YB-1 expression in primary tumors. Both proteins were predominantly expressed in the cytoplasm although in some cases they were also found in the nucleus. (b) Schematic of P-Akt and its associated proteins (IGF-1R, Her-2, EphA2, ILK, YB-1, and GFI-1) in breast cancer. These data led to the working model that YB-1 is an intermediate signaling molecule for the growth factor/Akt pathway. The solid arrows indicate that an association between proteins has been reported in cell-based models of breast cancer, whereas the broken lines represent anticipated relationships

there was minimal nonspecific binding of YB-1, P-Akt, or Akt to the IgG control (Figure 2a, lanes 3 and 4). Additionally, we determined that both P-Akt and YB-1 were present in the input lysates prior to immunoprecipitation (Figure 2a, lanes 5 and 6). We therefore further pursued the idea that Akt must be activated in order to bind to YB-1. An *in vitro* co-immunoprecipitation experiment was performed using recombinant YB-1 and activated Akt-1 or unactivated Akt-1. The recombinant proteins were incubated together and the complex was isolated with anti-Akt antibody. Activated Akt-1 co-immunoprecipitated with YB-1 (Figure 2b, lane 2) while inactive Akt-1 did not (Figure 2c, lane 2). Therefore, activated Akt-1 forms a complex with YB-1 both *in vivo* and *in vitro*.

YB-1 is made up of alanine/proline-rich domain (AP), CSD, and C-terminal domain (CT). CSD is involved in RNA and DNA binding (Kloks *et al.*, 2002); thus, it is

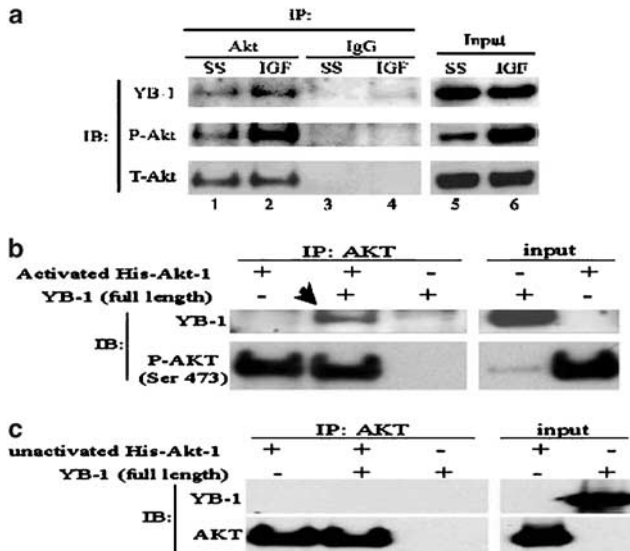


**Figure 2** Akt binds to YB-1 *in vivo* and *in vitro*. (a) MDA-MB-231 cells were either serum starved or stimulated for 30 min with IGF-1 and then proteins from the cytoplasmic fraction were immunoprecipitated with the 5G3 Akt antibody that binds to activated and unactivated forms of the protein. The majority of Akt in the complex with YB-1 appeared to be phosphorylated (lane 2, panel 2). Total Akt was further evaluated as a loading control (lanes 1 and 2, bottom panel). A portion of the input extract was evaluated to demonstrate that YB-1 and Akt were present in the samples prior to immunoprecipitation (lanes 5 and 6, top panel). (b) Activated recombinant Akt-1 (1  $\mu$ g) was incubated in the presence or absence of purified wild-type YB-1 (2  $\mu$ g) for 2 h and immunoprecipitated using the 5G3 Akt antibody *in vitro*. YB-1 was only present when the samples were incubated with activated Akt-1 (lane 2, arrow). The activated form of Akt-1 was confirmed by immunoblotting with the Ser473 antibody to Akt (lower panel). (c) Unactivated recombinant Akt-1 was incubated with YB-1 as described in (b). The membrane was immunoblotted for total Akt (lanes 1 and 2, bottom panel) to demonstrate that while the protein was present it failed to bind to YB-1. The input proteins were also confirmed (lanes 4 and 5)

believed to be critical for mediating gene expression changes. In addition, CSD participated in the trafficking of YB-1 from the cytoplasm to the nucleus (Jurcotta *et al.*, 2003). To identify where Akt binds to YB-1, we compared fusion proteins expressing the full-length YB-1 (GST-YB-1 (WT)), the AP domain (GST-YB-1 (AP)), and AP and CSD (GST-YB-1 (AP/CSD)) (Figure 3a). The fusion proteins were immobilized to resin, and binding assays were performed in the presence of activated recombinant Akt-1. From this experiment, we determined that activated Akt-1 only bound to GST-YB-1 fusion proteins that contain a CSD (Figure 3b, lanes 3 and 4). We confirmed that the input proteins were equal in the binding assay by analysing an aliquot of the extracts on an acrylamide gel stained with colloidal blue (Figure 3c). These results indicated that Akt binds the CSD of YB-1.

This prompted us to test whether or not YB-1 was indeed a phospho-substrate for Akt. To this effect, we ultimately determined that activated Akt-1 phosphorylated full-length YB-1 using an *in vitro* kinase assay

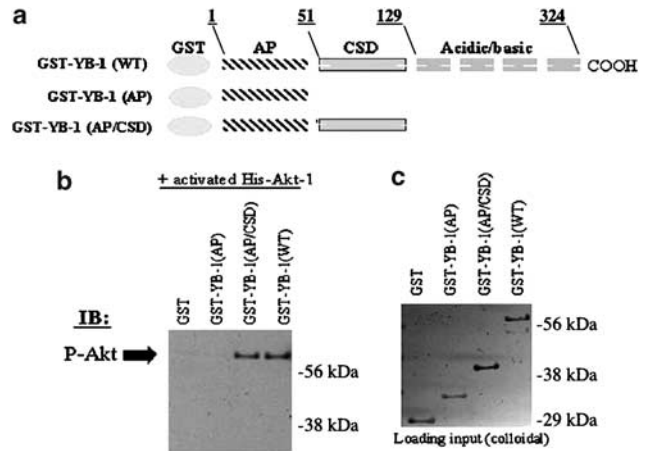


**Figure 3** Akt binds to the CSD on YB-1. (a) GST-tagged YB-1 deletion mutants were constructed to identify the region where P-Akt binds YB-1. Three GST-YB-1 fusion proteins were evaluated: GST-YB-1 (WT), GST-YB-1 (AP), and GST-YB-1 (AP/CSD). (b) Activated Akt-1 binds to GST-YB-1 and GST-YB-1 (AP/CSD). In contrast, the fusion protein expressing the AP domain alone was unable to interact with Akt. (c) An aliquot of each of the fusion proteins was evaluated on an acrylamide gel stained with colloidal blue to confirm that they were equally expressed

(Figure 4a, lane 1). Importantly, it was noted that one major phospho-protein was resolved by gel electrophoresis when YB-1 was incubated with activated Akt-1 (Figure 4a, lane 1). We also determined that unactivated Akt-1 did not phosphorylate YB-1 (Figure 4a, lane 2). From this point, we focused on the possibility that Akt may phosphorylate CSD. Using GST fusion proteins for the AP and/or CSD domains, we determined that Akt only phosphorylates those with an intact CSD (Figure 4b). An aliquot of each of the fusion proteins was also visualized on a colloidal blue-stained gel to confirm that the samples were loaded equally (Figure 4c). Next, a fusion protein expressing only the YB-1 CSD was generated first to show that Akt phosphorylates just this domain. We also used the CSD(wt) and CSD mutants to map the Akt phosphorylation site. Based upon the protein sequence of CSD, Thr80 and Ser102 were the most likely candidate phosphorylation sites because they resembled the RxRxxS/T recognition sequence to some degree (Figure 5a). In addition, five other threonine sites are present on CSD (Thr56, Thr62, Thr89, Thr106, and Thr125) that could be potentially phosphorylated by Akt but are less likely given they are not flanked by the sequence described above. First we demonstrated that Akt-1 directly phosphorylated the GST:CSD fusion protein (Figure 5b). Following this observation, we systematically mutated each of the serine and threonine sites on CSD to alanine in order to determine where Akt-1 phosphorylation occurs. The loss of Ser102 inhibited phosphorylation by Akt-1 while mutation of Thr80 did not (Figure 5b). Similarly, loss of the other Thr sites did not inhibit phosphorylation by Akt (data not shown). Based on the titration of the wild-type CSD that was phosphorylated by Akt-1, we estimated that

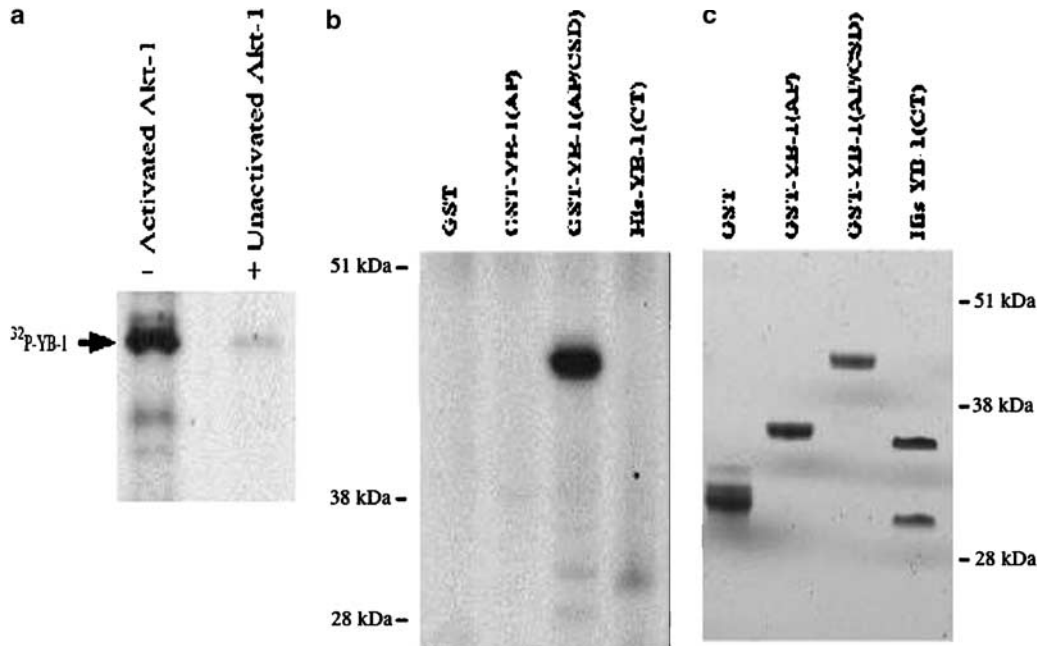


**Figure 4** Akt-1 directly phosphorylates full-length YB-1. (a) Activated Akt-1 was incubated with full-length human recombinant YB-1 in the presence of [ $\gamma$ - $^{32}$ P]ATP. One major phosphorylation product was detected (lane 1, arrow). Introduction of unactivated Akt-1 did not appreciably phosphorylate YB-1 (lane 2). (b) Activated Akt-1 (1  $\mu$ g) was incubated with 2  $\mu$ g GST, GST-YB-1 (AP), GST-YB-1 (AP/CSD), His-YB-1 (CT), or GST-YB-1 (WT) in the presence of [ $\gamma$ - $^{32}$ P]ATP. The GST-YB-1 (AP/CSD) and the GST-YB-1 (WT) fusion proteins were phosphorylated by activated recombinant Akt-1. In contrast, the fusion protein lacking CSD (GST-YB-1 (AP)) was not phosphorylated in the presence of activated Akt-1. (c) Equal loading of GST-YB-1 fusion proteins, His-YB-1, and GST alone was verified by colloidal blue staining

mutating Ser102 inhibited phosphorylation by >75% (Figure 5b). As a control, we determined that unactivated Akt-1 did not phosphorylate the GST fusion proteins (data not shown). The fusion proteins were confirmed to be YB-1 by Western blotting using a polyclonal antibody that recognizes CSD (Figure 5c). In addition, we determined that activated Akt-1 still binds to the GST:CSD(Ala102) mutant (Figure 5d, top panel, lane 2) even though phosphorylation is impaired. Activated Akt-1 bound to GST:CSD(wt) and GST:CSD(Ala102) with similar affinity (Figure 5d, lanes 1 and 2). The sample loading was controlled for by reprobing for total Akt (Figure 5d, bottom panel, lanes 1 and 2). We also confirmed that unactivated Akt-1 does not bind to GST:CSD(wt) or GST:CSD(Ala102) (Figure 5d). From these data, we concluded that only activated Akt-1 phosphorylates YB-1 on CSD at Ser102. A question that then arises is whether there are one or more Akt phosphorylation sites on YB-1. We suspect that there is only one site because a single product was evident in the kinase assays using either full-length YB-1 or CSD. To examine this further, we took a bioinformatics approach using Motif scanner, which is a publicly available website for predicting protein : protein interactions (<http://scansite.mit.edu>). The results from Motif Scanner predicted that YB-1 has only one Akt phosphorylation site using low stringency and it is located at Ser102 (data not shown). We used low-stringency criteria for this study because we wanted to find any potential phosphorylation site(s). Henceforth,

using bioinformatics and a predictive algorithm, we independently determined that Akt likely phosphorylates YB-1 on a single site, which is located at Ser102. It was noted that the location of YB-1(Ser102) is outside of the ribonucleoprotein-1 (RNP-1) and ribonucleoprotein-2 (RNP-2) binding motifs, which is the principal site for RNA interactions (Figure 5e). This suggested to us that phosphorylation of YB-1 at Ser102 probably does not have a direct impact on RNA binding. On a structural basis, the location of YB-1(Ser102) is in a flexible loop region, indicating that it may be accessible to the crevice formed by Akt-1 when it is in an active conformation (Figure 5f). The flexible loop region of YB-1 is adjacent to the RNA and DNA binding surfaces; therefore, phosphorylation may alter the conformation of CSD and thereby change the way it interacts with nucleic acids.

It is noteworthy that the Akt phosphorylation site on YB-1 is not flanked by a conventional RxRxxS/T motif. The Akt phosphorylation site on YB-1 is rather RxxxxS. This observation adds new possibilities for the discovery of additional substrates. Much of our understanding of how Akt functions at the molecular level comes from studies designed to find candidate substrates based upon the idea that it binds to an RxRxxS/T. Using the RxRxxS/T motif as a benchmark, several Akt substrates have been identified. One of the first Akt substrates identified was forkhead transcription factor L1 (Brunet *et al.*, 1999). Likewise, the Akt binding partners AFX (Kops *et al.*, 1999) and glycogen synthase kinase 3

(GSK) (van Weeren *et al.*, 1998) among several others were identified accordingly. Putative Akt kinase substrates are also proposed by screening phage libraries with a synthetic RxRxxS/T peptide (Obata *et al.*, 2000).

There are however Akt substrates that do not have classic RxRxxS/T motifs. For example, the transcription factors CREB (Du and Montminy, 1998) and BRCA-1 (Altioek *et al.*, 1999) are Akt substrates that do not possess these sequences. Thus, we anticipate that like YB-1 there are additional Akt substrates with non-conserved binding motifs some of which may have important implications in cancer.

*Loss of the Akt phosphorylation site on YB-1 suppresses tumor growth and nuclear translocation*

Once the phosphorylation site was mapped on the CSD motif, full-length YB-1 was subsequently mutated at Ser102 > A102 and expressed in MCF-7 cells. Comparisons were made to cells expressing wild-type YB-1. The cells expressing the empty vector (EV), YB-1, or YB-1(Ala102) were 3 × Flag tagged to monitor transgene expression. The transgene expression was approximately equal to endogenous YB-1. This was determined by using an anti-YB-1 antibody that recognizes both recombinant and endogenous YB-1 (Figure 6a). The stable cell lines were then plated in soft agar and examined for differences in their ability to form colonies after 21 days. The MCF-7(YB-1) cells developed approximately twice the number of colonies in soft agar compared to MCF-7(Ala102) (Figure 6b). Moreover, the size of the colonies that developed from the MCF-7(YB-1) cells was notably larger than those that arose from either MCF-7(EV) or MCF-7(Ala102) (Figure 6c). We also noted that the cells expressing MCF-7(Ala102) produced even smaller colonies than those expressing MCF-7(EV), suggesting that the mutant potentially had a dominant-negative effect on endogenous YB-1. Tumor cell growth was also enhanced by the expression of YB-1 in the presence of serum under monolayer culture conditions (Figure 6d). In contrast, the expression of

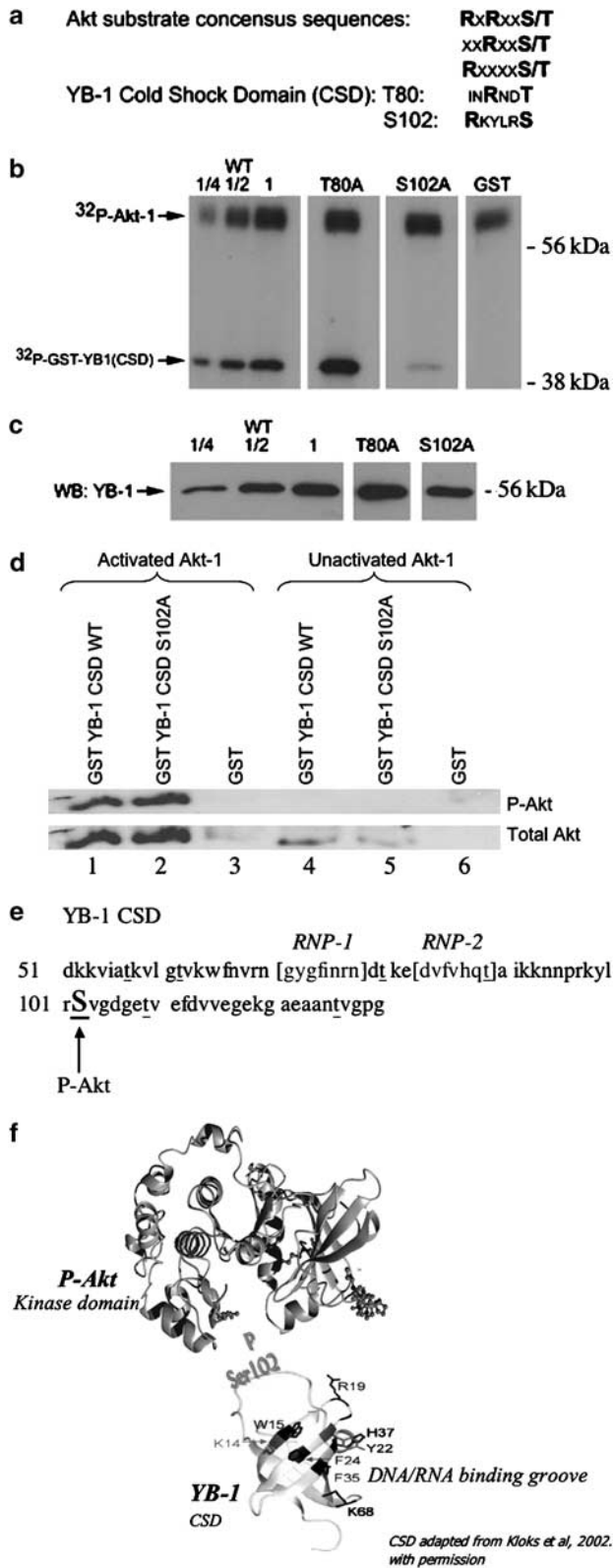


**Figure 5** The Akt phosphorylation site on the YB-1 CSD is located at Ser102. (a) The Akt consensus sequences were aligned with the two most probable phosphorylation sites on YB-1, which were Thr80 and Ser102. (b) *In vitro* kinase assays were performed on just CSD and not the other domains in the presence of activated Akt-1. Increasing amounts of the product were analysed to assess linearity of detection. CSD was mutated at either Thr80 > Ala80 or Ser102 > Ala102 and the *in vitro* kinase assay was performed in the presence of recombinant Akt-1. CSD was titrated to estimate the loss of phosphorylation. (c) The recombinant protein produced by the bacteria was examined for YB-1 expression by immunoblotting. (d) GST:CSD(wt) and GST:CSD(A102) were incubated with activated (lanes 1–3) or unactivated Akt-1 (lanes 4–6) and *in vitro* binding assays were performed. The blots were probed initially for P-Akt (top panel). As a negative control, GST was incubated with activated or unactivated Akt-1 (lanes 3 and 6, respectively). The immunoblot was re-probed with an antibody to total Akt (bottom panel). (e) Location of each of the serine and threonine sites on the CSD of YB-1 (underlined). Each of these sites was mutated to alanine using site-directed mutagenesis to determine where phosphorylation by Akt occurs. The proximity of YB-1(Ser102) to RNP-1 and RNP-2 is also depicted. (f) The crystal structures of the Akt kinase domain in its active conformation and the YB-1 CSD indicate that the YB-1(Ser102) site is located in a flexible loop region accessible to the kinase

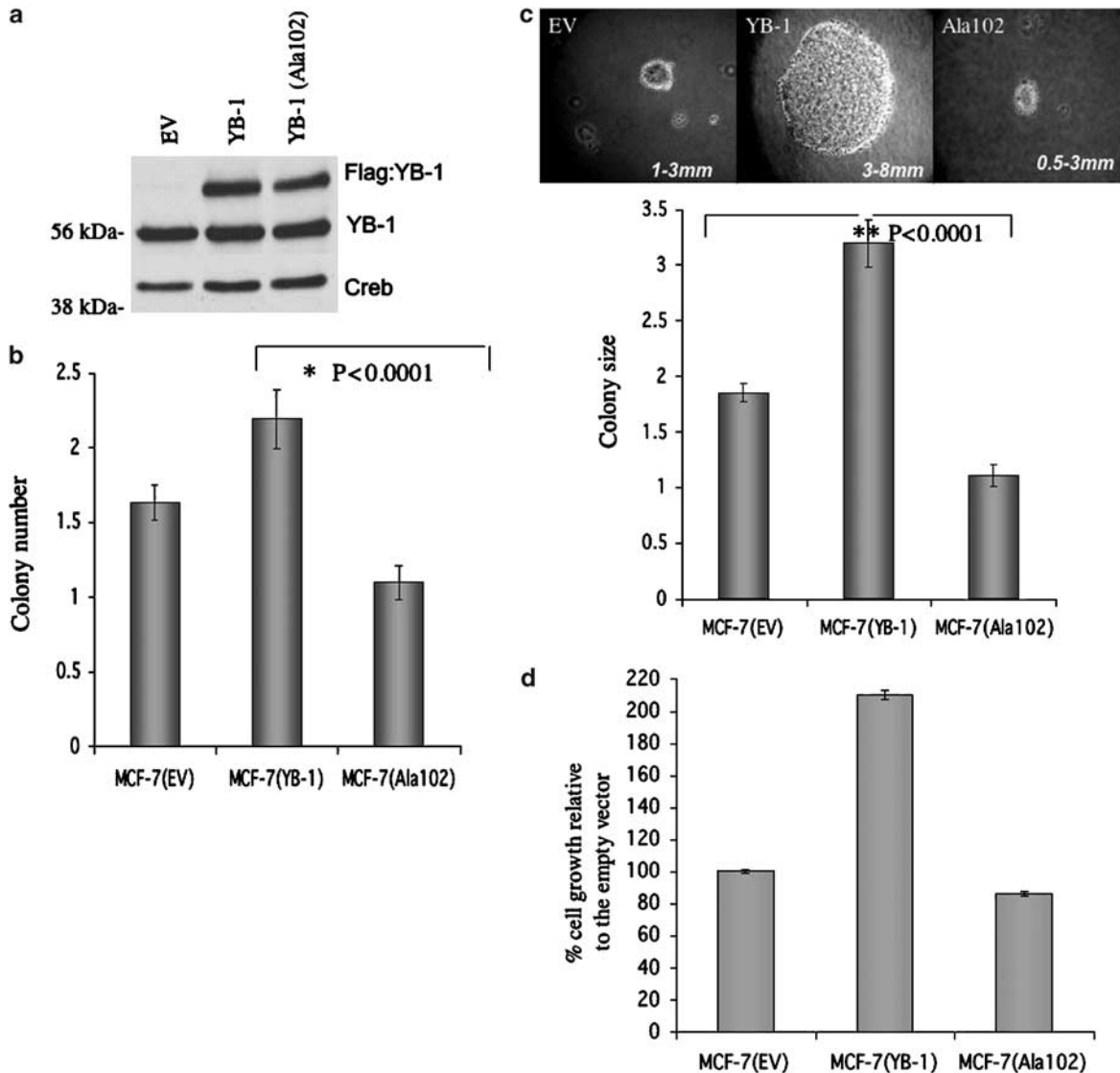


**Figure 6** Disruption of the YB-1(102) site perturbs tumor cell growth. (a) Characterization of exogenous and endogenous YB-1 expression in the MCF-7 cells by immunoblotting. The exogenous YB-1 transgenes were Flag tagged to monitor expression and their levels were compared between MCF-1(EV), MCF-1(YB-1), and MCF-7(YB-1:Ala102) (lanes 1–3, respectively). The addition of the 3 × Flag epitope increased the size of the recombinant protein from ~56 to ~59 kDa. Recombinant and endogenous YB-1 proteins were thereby identified using an anti-YB-1 antibody. Creb was evaluated as a loading control (bottom panel). (b) MCF-7 cells were transfected with either EV, YB-1(wt), or YB-1(Ala102) and stable pooled clones were then examined for differences in anchorage-independent growth. The MCF-7(EV), MCF-7(YB-1), and MCF-7(Ala102) cells expressed on average 1.6, 2.19, and 1.09 colonies per field, respectively. (c) The MCF-7(EV), MCF-7(YB-1), and MCF-7(Ala102) cells grew into colonies that were 1.85, 3.19, and 1.10 mm in size on average. Representative photomicrographs are included to illustrate the remarkable differences in colony size (inset). The number of colonies was quantified by counting random fields ( $n = 33$ ) for each cell line, while the size was determined using an eyepiece with an ocular scale. The statistical significance was determined using the Student's *t*-test. (d) The growth of tumor cells in monolayer was addressed in the presence of serum (5% FBS/RPMI 1640). MCF-7 cells expressing either EV, YB-1(wt), or YB-1(Ala102) were compared. Cell growth was evaluated after 48 h and viability was measured using Trypan blue exclusion. Each condition was evaluated in replicates of four, and statistical significance was determined using the Student's *t*-test. YB-1 enhanced monolayer growth in the presence of serum compared to either the EV- or YB-1(102)-expressing cells,  $P < 0.001$

YB-1(Ala102) did not result in enhanced cell growth in monolayer.

We then questioned whether or not the Akt phosphorylation site on YB-1 altered nucleocytoplasmic trafficking. Flag:YB-1 was distributed equally between the cytoplasm and the nucleus whereas Flag:YB-1(Ala102) was retained in the cytoplasm (Figure 7a).

This was determined using either anti-YB-1 (Figure 7a, first panel) or anti-Flag (Figure 7a, second panel) to detect the recombinant proteins. It was also noted that expression of MCF-7(Ala102) decreased the amount of detectable endogenous YB-1 in the nucleus, suggesting that it may have a dominant-negative effect (Figure 7a, third panel). The intensity of Flag:YB-1 and

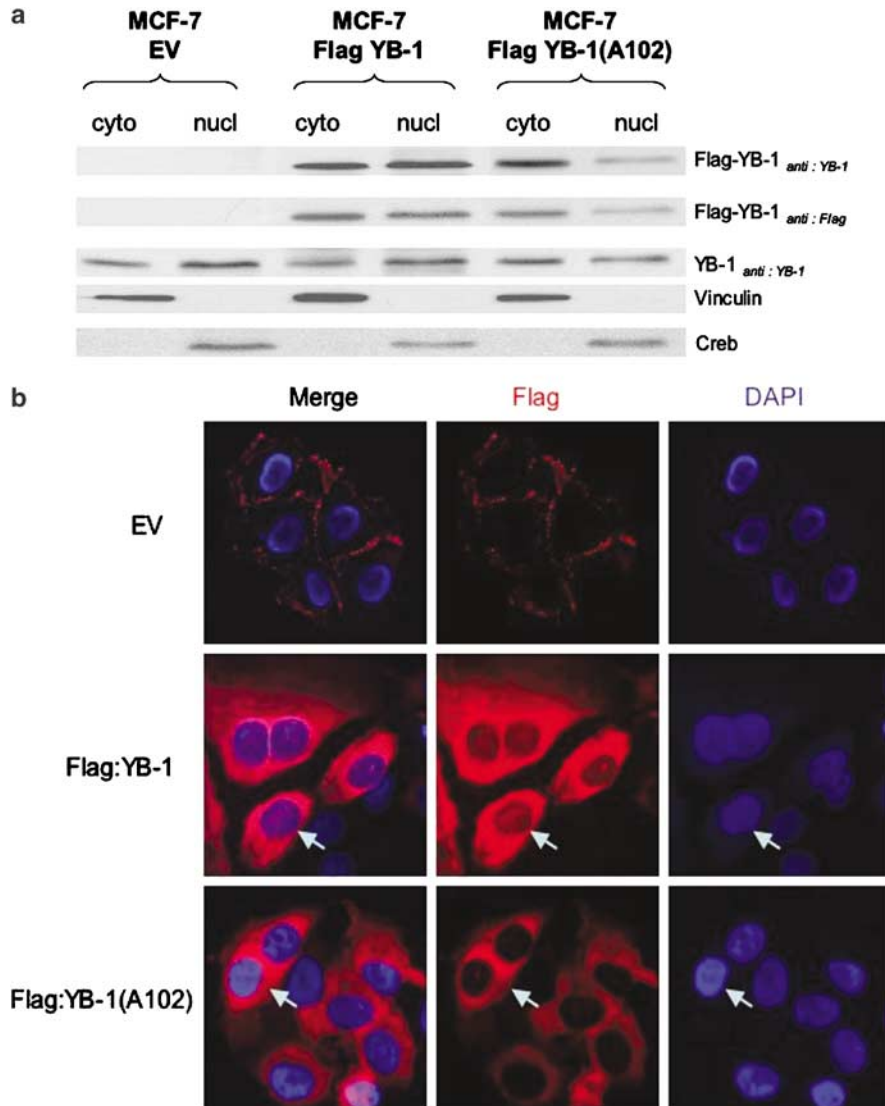


**Figure 7** Disruption of YB-1(Ser102) alters nuclear localization. **(a)** The localization of Flag:YB-1 and Flag:YB-1(Ala102) was evaluated by fractionating proteins from the cytoplasmic and nuclear compartments. Anti-YB-1 (first panel) and anti-Flag (second panel) were used to identify the proteins. Endogenous YB-1 was also detected (third panel). The purity of the cytoplasmic and nuclear fractions was monitored using anti-vinculin (fourth panel) and creb (fifth panel). The differences in YB-1 and YB-1(Ala102) expression in the nucleus were not due to sample loading because creb was equally detected in the samples (fifth panel). **(b)** The subcellular localization of Flag:YB-1 and Flag:YB-1(Ala102) was also examined by immunofluorescence. MCF-7 cells expressing either EV, Flag:YB-1, or Flag:YB-1(Ala102) were evaluated using an anti-Flag antibody, which was visualized with Texas red (center images). The nuclei were stained with DAPI (right images). The localization of Flag:YB-1 in the nuclei is evident in the merged image (left image). The cells were plated at 50–60% confluence and the images were captured at  $\times 400$  magnification

Flag:YB-1(Ala102) bands was evaluated using densitometry to quantify the relative amounts of the recombinant proteins in the cytoplasmic and nuclear fractions. The nuclear/cytoplasmic ratios for Flag:YB-1 and Flag:YB-1(Ala102) were 1.23 and 0.41, respectively, when the proteins were detected by anti-YB-1. Likewise, the nuclear/cytoplasmic ratios for Flag:YB-1 and Flag:YB-1(Ala102) were 0.99 and 0.63, respectively, when quantification was based on the signal produced by anti-Flag. These data indicated that mutation of the Akt phosphorylation site on YB-1 perturbed the nucleocytoplasmic shuttling of YB-1 under log growing

conditions. To evaluate this at the cellular level, the distribution of recombinant Flag:YB-1 and Flag:YB-1(Ala102) was examined by immunofluorescence. In the presence of serum, Flag:YB-1 was detected both in the cytoplasm and in the nucleus (Figure 7b, middle panel). However, mutant Flag:YB-1(Ala102) was abundantly expressed in the cytoplasm but not in the nucleus (Figure 7b, bottom panel). MCF-7 cells expressing EV were also evaluated as a negative control for the Flag antibody (Figure 7b, top panel). There was a small amount of nonspecific staining on the plasma membrane but not throughout the cytoplasm or nucleus, thus the

anti-Flag staining appeared to be specific for the recombinant YB-1 proteins. From these studies, we concluded that YB-1 regulates tumor growth and its presence in the nucleus may be important for mediating this effect.

We concluded from these results that YB-1 plays a role in tumor cell growth and this is consistent with its effects on pre-neoplastic breast epithelial cells (Jurchott *et al.*, 2003). In that study, YB-1 was linked to an increase in cell cycle progression when cells were grown in monolayer. The research was conducted using the HBL100 cells that are a model of pre-neoplastic breast cancer. They did not address whether YB-1 also stimulated growth in soft agar most likely because the HBL100 cells do not form colonies in agar, which is consistent with our own studies (unpublished). We have therefore been able to advance the field by showing that YB-1 enhances the transforming properties of breast cancer cells and that the Akt phosphorylation site is particularly important for the growth of the colonies.

The way in which Akt regulates oncogenes such as YB-1 is of interest because it helps us to begin to understand how this commonly expressed kinase facilitates tumor cell growth. Our data support the idea that Akt and YB-1 work together to promote the growth and possibly the development of breast tumors, although more work is necessary to prove this point definitively. This is in contrast to a recent report indicating that YB-1 has tumor suppressive effects in chicken embryo fibroblasts by perturbing Akt-mediated transformation (Bader *et al.*, 2003). We suspect that the differences lie in the cellular systems under investigation. With respect to breast cancer, the preferential expression of YB-1 in human tumors argues against it being a tumor suppressor. For example, YB-1 is preferentially expressed in breast cancer relative to normal tissue (Rubinstein *et al.*, 2002). YB-1 also correlates with poor survival for patients with breast cancer (Janz *et al.*, 2002). Importantly, that study also indicated that the expression of YB-1 related to an increased risk of relapse (Janz *et al.*, 2002). Taken together, the weight of evidence thus points toward YB-1 as a potentially important oncogene in breast cancer.

Based upon our work, YB-1 is now placed in the Akt signal transduction pathway. Thus, we have identified a new member of the Akt signaling network. In addition, we defined the relationship between Akt activation and the expression of IGF-1R, HER-2, and ILK for the first time in patient samples. These relationships were previously appreciated only using experimental models. For example, MCF-7 breast cancer cells engineered to overexpress HER-2 exhibit an increase in Akt kinase activity, leading to resistance to chemotherapy (Knuefermann *et al.*, 2003). IGF-1R has also been shown to signal through Akt in cell-based models of breast cancer (Oh *et al.*, 2002). Finally, cell culture models support a role for ILK in the phosphorylation of Akt on serine 473 (Delcommenne *et al.*, 1998). In further support of this relationship, ILK knockout by either RNA interference or the Cre-Lox system results in significant inhibition of P-Akt and also Akt kinase activity (Troussard *et al.*,

2003). Thus, our data support cell-based models of growth factor-mediated signal transduction leading to Akt activation. We also found P-Akt to be related to the expression of EphA2, GFI-1, and YB-1, which have not been implicated in P-Akt signaling prior to this work. This point demonstrates the potential for TMAs as a hypothesis-generating tool, useful in exploring coordinate expression of signaling molecules in a large number of tumor samples. Thus, this study has identified patients who may benefit from therapies inhibiting P-Akt and has also expanded our knowledge of the Akt signaling network in primary tumors. From this initial screen, we identified YB-1 as a potential P-Akt binding partner. We conclude from our study that YB-1 is a novel substrate for Akt and propose that disrupting the interaction between these molecules could lead to new strategies for cancer intervention.

## Materials and methods

### *Patient information and tissue microarray construction*

For construction of TMA, 481 primary breast cancer samples were obtained from archival cases at Vancouver General Hospital between 1974 and 1995. Patient information and tumor pathology are summarized in Supplementary Table 2. Tumor samples were taken prior to initiation of cancer treatment, and were formalin-fixed and embedded in paraffin. A hematoxylin- and eosin-stained section of each tumor block was used to define and mark representative tumor regions. This section served as a guide for the selection of two 0.6 mm punches from each original tumor block, which were transferred to three composite recipient array blocks using a Tissue Micro Arrayer (Beecher Instruments, Sliver Springs, MD, USA) as previously described (Makretsov *et al.*, 2004). Serial 4- $\mu$ m-thick sections of the arrays were cut using a Leica microtome (Leica Microsystems, Nussloch, Germany) and mounted onto charged polylysine-coated glass slides. For P-Akt staining, the sections were first deparaffinized in xylene and rehydrated in graded ethanol solutions. Antigen retrieval was achieved by incubating the slides for 30 min in 10 mM citrate buffer (pH 6.0) in a vegetable steamer. Endogenous peroxidases were quenched by incubating the sections for 10 min in 3% H<sub>2</sub>O<sub>2</sub> diluted in water. Prior to application of the primary antibody, nonspecific interactions were blocked for 30 min using a nonserum blocking reagent (DAKO, Denmark), followed by 20 min with an avidin/biotin blocking solution (DAKO). The primary antibody (Phospho-AKT S473 IHC Specific, Cell Signaling Technologies (CST), Beverly, MA, USA) was diluted 1:250 with a 1% BSA solution, applied to the slides, and incubated overnight at 4°C. For signal amplification, we used the LSAB+ System (DAKO), which involved incubation with a biotinylated secondary antibody followed by streptavidin treatment. Signal was visualized by addition of NovaRed substrate (Vector Laboratories, Burlingame, CA, USA). Sections were counterstained with hematoxylin. Additionally, a negative control reaction without primary antibody was also performed for each TMA slide in parallel. To detect YB-1, the tissues underwent antigen retrieval in a citrate buffer, and then the slides were incubated with anti-YB-1 (1:2000 dilution, C-terminal epitope, from Dr Colleen Nelson). Details on the staining protocols for all the other proteins are available on our website <http://www.gpe-c.ubc.ca>. The images were viewed using the WebSlide Browser

program (Bacus Laboratories), which are available on our website.

#### *TMA scoring and data analysis*

Two pathologists and a basic scientist arrived at a consensus score for each core on TMA. The scoring system for P-Akt and YB-1 expression was as follows: (0) negative, (1) weak, (2) moderate, and (3) high staining intensity. Univariate correlation analysis between markers on TMA was performed using Fisher's exact test. Data were considered significant when  $P < 0.05$ .

#### *Cell lines and reagents*

The MDA-MB-231 and MCF-7 breast cancer cell lines were obtained from the American Type Culture Collection (Manassas, VA, USA). Long-range IGF-1 was from Diagnostic Systems Laboratories (Webster, TX, USA). The rabbit polyclonal anti-Akt (total), anti-P-Akt (Ser473), and anti-Akt (5G3) antibodies and the Akt kinase assay components were purchased from CST. The 5G3 antibody was used because it is a pan-Akt antibody. Additionally, it binds to both phosphorylated and unphosphorylated Akt. The polyclonal anti-YB-1 antibody (C-terminal epitope; Gimenez-Bonafe *et al.*, 2004) and a human YB-1 plasmid were provided by Dr Colleen Nelson (British Columbia Cancer Agency, Vancouver, Canada). To detect the CSD portion of YB-1, we used an anti-rabbit antibody (provided by Dr Valentina Evdokimova, University of British Columbia). Anti-rabbit protein G-agarose and glutathione-Sepharose beads were purchased from Pharmacia Biotech (St Louis, MO, USA). Leupeptin, aprotinin, sodium orthovanadate, and okadaic acid were obtained from Sigma (St Louis, MO, USA). Recombinant His-tagged activated and unactivated Akt-1 was purchased from Upstate Ltd (Lake Placid, NY, USA).

#### *Immunoprecipitations*

MDA-MB-231 cells were either serum starved or stimulated with IGF-1 for 30 min. Cytoplasmic and nuclear proteins were then isolated as previously described (Oh *et al.*, 2002). The cytoplasmic proteins (1 mg) were precleared by incubation with IgG-protein G beads for 2 h at 4°C. The precleared cellular extracts were incubated with anti-AKT (5G3; Cell Signaling) antibody for 24 h at 4°C. IgG antibodies were used for the negative controls. Proteins were separated using Nupage 4–12% gels following the manufacturer's protocol (Invitrogen). Membranes were then probed via Western blot using anti-Akt, anti-P-Akt, or anti-YB-1 antibodies.

#### *In vitro binding assays*

GST fusion proteins were constructed by cloning either full-length YB-1 or the individual domains (AP, AP/CSD, CSD, or CT) into a pGEX-4T-1 vector (AMRAD Corp., Victoria, Australia). The plasmids were expressed in JM105 *Escherichia coli* and induced to express the fusion proteins with 1.0 mM isopropyl- $\beta$ -D-thiogalactoside for 5 h at 37°C. For *in vitro* binding assays, 1  $\mu$ g of activated or unactivated His-Akt-1 (Upstate Biotechnology) was incubated with 2  $\mu$ g of the YB-1 fusion proteins in 400  $\mu$ l of lysis buffer for 2 h at 4°C. Akt-1 was immunoprecipitated with the 5G3 antibody. The resulting complex was immunoblotted for YB-1 expression. For YB-1 immunoprecipitation experiments, 1  $\mu$ g of the GST-YB-1 fusion proteins was prebound to GST-Sepharose resin. Activated His-Akt-1 (1  $\mu$ g) was then added to 400  $\mu$ l of MTPBS buffer (50 mM NaPO<sub>4</sub>, pH 7.5, 150 mM NaCl,

10 mM EDTA, pH 7.9, 1% v/v Triton X-100, 2 mM dithiothreitol (DTT), and protease inhibitors) for 2 h at 4°C. Proteins were separated on 4–12% Nupage gradient gels, transferred to nitrocellulose membranes, and probed by Western blot using anti-Akt and anti-YB-1 antibodies.

#### *In vitro kinase assays*

Phosphorylation of YB-1 was determined by incubating the activated His-Akt-1 (Upstate) with 2  $\mu$ g of recombinant YB-1 in a 20  $\mu$ l reaction mixture containing 10 mM MgCl<sub>2</sub>, 2 mM DTT, 5 mM  $\beta$ -glycerolphosphate, 0.1 mM Na<sub>3</sub>VO<sub>4</sub>, 25 mM Tris-HCl, pH 7.5, 100  $\mu$ M ATP, and 50  $\mu$ Ci [ $\gamma$ -<sup>32</sup>P]ATP. Reactions were incubated at 30°C for 30 min and then stopped by the addition of Laemmli's sample buffer. The proteins were subsequently resolved by 12% SDS-PAGE and analysed by autoradiography. Alternatively, to map the site of phosphorylation on YB-1, GST-CSD (2  $\mu$ g) was incubated with 1  $\mu$ g of recombinant activated His-Akt-1 (Upstate) and *in vitro* kinase assays were performed.

#### *Site-directed mutagenesis*

Site-directed mutagenesis was performed according to the manufacturer's protocol (Stratagene, Windsor, ON, USA). Thr<sup>80</sup> and Ser<sup>102</sup> on YB-1 were replaced with alanine in the GST-YB-1(CSD) vector using the following primers: T80A, 5'-CTCAACAGGAATGACGCCAAGGAAGATG-3'; S102A, 5'-GGAAGTACCTTCGCGCTGTAGGAGATGG-3'. PCR conditions were as follows: 95°C for 1 min followed by 18 cycles of 94°C for 20 s, 55°C for 1 min, 68°C for 6 min, and 68°C for 10 min. PCR reactions were then incubated with *DpnI* for 1 h at 37°C and 1  $\mu$ l was used to transform TOP-10 bacteria (Invitrogen). All resultant vectors were sequence verified for the respective mutation.

#### *Anchorage-independent growth*

YB-1 or YB-1(Ala102) was cloned into the 3  $\times$  Flag-CMV-10 vector (Sigma) using *HindIII* and *XbaI* restriction sites. These plasmids along with EV were transfected into MCF-7 cells using Transfectamine 20000 (Invitrogen). Stable pooled clones were established and transgene expression was confirmed by immunoblotting using the Flag M2 monoclonal (Sigma) as well as YB-1 polyclonal antibodies (gift from Dr Colleen Nelson). Flag:YB-1 and Flag:YB-1(Ala102) pooled clones that expressed equivalent levels of the transgenes were used for subsequent studies. The levels of Flag:YB-1 and Flag:YB-1(Ala102) expression was also examined relative to endogenous YB-1. We were able to easily distinguish Flag:YB-1 from endogenous YB-1 using the anti-YB-1 antibody because the addition of the 3  $\times$  Flag increased the size of the recombinant protein from ~56 to ~59 kDa. Recombinant and endogenous YB-1 proteins were approximately equivalent based on immunoblotting with the antibody to YB-1. Cells were plated in soft agar as previously described (Dunn *et al.*, 1998). The only modification was that the top layer was 0.4% and the bottom layer was 0.8%. Colonies were allowed to grow for 21 days. Each cell line was plated in replicates of six. To quantify the number of colonies, random fields ( $n = 4$ /plate) were counted. The size of the colonies was estimated using a microscope with an ocular grid equipped with a scale. Statistical differences were determined using the Student's *t*-test. Cell growth in monolayer was evaluated by plating 20 000 cells in a 24-well dish. The next day, the cells were either serum starved or given 5% FBC/RPMI for 48 h. Cell viability was measured by Trypan blue exclusion.

### Subcellular localization of YB-1

The MCF-7 cells expressing EV, Flag:YB-1, or Flag:YB-1(Ala102) were plated at 70% confluence in the presence of 5% FBS/RPMI 1640. Cytoplasmic and nuclear fractions were then isolated. Briefly, cells were lysed in buffer A (10 mM HEPES (pH 7.9), 1.5 mM MgCl<sub>2</sub>, 1 mM EDTA, 10 mM KCl, 0.1% v/v NP-40, 2.5 mM sodium pyrophosphate, 1 mM β-glycerolphosphate, 1 mM sodium vanadate, 1 μg/ml leupeptin and aprotinin, 1 mM PMSF, and 100 nM okadaic acid) for 10 min. Cells were then sheared using a 22-gauge needle and centrifuged at 10 000 r.p.m. for 2 min. The supernatant fractions (cytoplasmic soluble proteins) were collected. The nuclear pellet was then washed once in buffer B (10 mM Tris-HCl pH 7.2, and 2 mM MgCl<sub>2</sub>) and then lysed in buffer C (0.42 mM NaCl, 20 mM HEPES pH 7.9, 1.5 mM MgCl<sub>2</sub>, 20% v/v glycerol, 2.5 mM sodium pyrophosphate, 1 mM β-glycerolphosphate, 1 mM sodium vanadate, 1 μg/ml leupeptin and aprotinin, 1 mM PMSF, and 100 nM okadaic acid). Lysates were incubated on ice for 30 min, sheared using a 26-gauge needle, and then centrifuged for 20 min at 10 000 r.p.m. Once the cytoplasmic and nuclear fractions were collected, we evaluated the isolates for Flag:YB-1 and Flag:YB-1(Ala102). The proteins were evaluated using antibodies to YB-1 or to Flag. Vinculin (1:1000 dilution, CST) and creb (1:1000 dilution, CST) were also examined as cytoplasmic and nuclear markers, respectively. The vinculin and creb proteins were detected using anti-mouse and anti-rabbit secondary antibodies (diluted 1:10 000), respectively. The subcellular localization of Flag:YB-1 and Flag:YB-1(Ala102) was also examined by immunofluorescence. MCF-7 cells expressing either EV, Flag:YB-1, or Flag:YB-1(Ala102) were plated on coverslips

at 50–60% confluence in the presence of 5% FBS/RPMI 1640 and allowed to attach overnight. After 2 days, cells were fixed with 2% paraformaldehyde in PBS for 20 min, washed with PBS, and then permeabilized with 0.1% Triton X-100 in PBS for 10 min at room temperature. The anti-Flag M2 monoclonal antibody (Sigma) was used at a concentration of 20 μg/ml (1:500) and visualized with Texas red fluorescence-conjugated secondary antibody (goat anti-mouse) diluted 1:500. The nuclei were stained with Vectashield (Vector Laboratories, Burlingame, CA, USA), a DAPI-containing mounting medium. Cellular images were captured on a Zeiss fluorescence microscope at ×400 magnification.

### Acknowledgements

We thank Dr Marty Cathcart for helping us with the Motif Scanner search engine. Dr Pepita Gimenez-Bonafe is gratefully recognized for creating the human YB-1 construct. We also thank Dr Brad McLean for helping us render the Akt-1 kinase structure using the RasMol program. M Chen is a visiting scholar in the Department of Pediatrics, University of British Columbia. SED and CKP are recipients of Investigatorship Awards from the BC Research Institute for Children's and Women's Health. This study was supported by the Canadian Breast Cancer Research Alliance through the National Cancer Institute of Canada-Streams of Excellence Program, the Johal Basic and Translational Research Program for Pediatric Oncology (SED and CJP), the Bertram Hoffmeister postdoctoral fellowship (BS), the BC Research Institute for Children's and Women's Health (SED and CJP), and the Canadian Institutes of Health Research (SED and CJP).

### References

- Altiock S, Batt D, Altiock N, Papautsky A, Downward J, Roberts TM and Avraham H. (1999). *J. Biol. Chem.*, **274**, 32274–32278.
- Bader AG, Felts KA, Jiang N, Chang HW and Vogt PK. (2003). *Proc. Natl. Acad. Sci. USA*, **100**, 12384–12389.
- Bargou RC, Jurchott K, Wagener C, Bergmann S, Metzner S, Bommert K, Mapara MY, Winzer KJ, Dietel M, Dorken B and Royer HD. (1997). *Nat. Med.*, **3**, 447–450.
- Brazil DP and Hemmings BA. (2001). *Trends Biochem. Sci.*, **26**, 657–664.
- Brunet A, Bonni A, Zigmond MJ, Lin MZ, Juo P, Hu LS, Anderson MJ, Arden KC, Blenis J and Greenberg ME. (1999). *Cell*, **96**, 857–868.
- Delcommenne M, Tan C, Gray V, Rue L, Woodgett JR and Dedhar S. (1998). *Proc. Natl. Acad. Sci. USA*, **95**, 11211–11216.
- Du K and Montminy M. (1998). *J. Biol. Chem.*, **273**, 32377–32379.
- Dunn SE, Ehrlich M, Sharp NJH, Reiss K, Solomon G, Hawkins R, Baserga R and Barrett JC. (1998). *Cancer Res.*, **58**, 3353–3361.
- Dunn SE, Torres JV and Barrett JC. (2001). *Cancer Res.*, **61**, 1367–1374.
- Feng J, Park J, Cron P, Hess D and Hemmings BA. (2004). *J. Biol. Chem.*, **279**, 41189–41196.
- Gimenez-Bonafe P, Fedoruk MN, Whitmore TG, Akbari M, Ralph JL, Gleave ME and Nelson CC. (2004). *Prostate*, **59**, 337–349.
- Grant CE and Deeley RG. (1993). *Mol. Cell. Biol.*, **13**, 4186–4196.
- Higashi K, Inagaki Y, Fujimori K, Nakao A, Kaneko H and Nakatsuka I. (2003). *J. Biol. Chem.*, **278**, 43470–43479.
- Hill MM and Hemmings BA. (2002). *Pharmacol. Ther.*, **93**, 243–251.
- Janz M, Harbeck N, Dettmar P, Berger U, Schmidt A, Jurchott K, Schmitt M and Royer HD. (2002). *Int. J. Cancer*, **97**, 278–282.
- Jurchott K, Bergmann S, Stein U, Walther W, Janz M, Manni I, Paiggo G, Fietze E, Dietel M and Royer HD. (2003). *J. Biol. Chem.*, **278**, 27988–27996.
- Kamura T, Yahata H, Amada S, Ogawa S, Sonoda T, Kobayashi H, Mitsumoto M, Kohno K, Kuwano M and Nakano H. (1999). *Cancer*, **85**, 2450–2454.
- Kloks CPAM, Spronk CAEM, Lasonder E, Hoffmann A, Wuister GW, Grzesiek S and Hilbers CW. (2002). *J. Mol. Biol.*, **316**, 317–326.
- Knuefermann C, Lu YY, Liu B, Jin W, Liang K, Wu L, Schmidt M, Mills GB, Mendelsohn J and Fan Z. (2003). *Oncogene*, **22**, 3205–3212.
- Koike K, Uchiumi T, Toh S, Wada M, Kohno K and Kuwano M. (1997). *FEBS Lett.*, **417**, 390–394.
- Kops GJPL, de Ruiter ND, De Vries-Smits AMM, Powell DR, Bos JL and Burgering BMT. (1999). *Nature*, **398**, 630–634.
- Lasham A, Moloney S, Hale T, Homer C, Zhang Y, Murison JG, Braithwaite AW and Watson J. (2003). *J. Biol. Chem.*, **278**, 35516–35523.
- Makretsov N, Huntsman D, Nielsen T, Yorlida E, Peacock M, Cheang M, Dunn SE, Hayes M, van de Rijn M, Bajdik CD and Gilks B. (2004). *Clin. Cancer Res.*, **10**, 6143–6151.
- Nicholson KM and Anderson NG. (2002). *Cell. Signal.*, **14**, 381–395.
- Obata T, Yaffe MB, Leparac GG, Piro ET, Maegawa H, Kashiwagi A, Kikkawa R and Cantley LC. (2000). *J. Biol. Chem.*, **275**, 36108–36115.

- Oda Y, Ohishi Y, Saito T, Hinoshita E, Uchiumi T, Kinukawa N, Iwamoto Y, Kohno K, Kuwano M and Tsuneyoshi M. (2003). *J. Pathol.*, **199**, 251–258.
- Oda Y, Sakamoto A, Shinohara N, Ohga T, Uchiumi T, Kohno K, Tsuneyoshi M, Kuwano M and Iwamoto Y. (1998). *Clin. Cancer Res.*, **4**, 2273–2277.
- Oh JS, Buchel P, Martin K, Kucab JE, Oshimura T, Bennett L, Barrett JC, DiAugustine RP, Afshari C and Dunn SE. (2002). *Neoplasia*, **4**, 204–217.
- Okamoto T, Izumi H, Imamura T, Takano H, Ise T, Uchiumi T, Kuwano M and Kohno K. (2000). *Oncogene*, **19**, 6194–6202.
- Persad S, Attwell S, Gray V, Delcommenne M, Troussard A, Sanghera J, Walsh MP and Dedhar S. (2001). *J. Biol. Chem.*, **276**, 27462–27469.
- Rubinstein DB, Stortchevoi A, Bossalis M, Ashfaq R and Guillaume T. (2002). *Cancer Res.*, **62**, 4985–4991.
- Shibao K, Takano H, Nakayama Y, Okazaki K, Nagata N, Izumi H, Uchiumi T, Kuwano M, Kohno K and Itoh H. (1999). *Int. J. Cancer*, **83**, 732–737.
- Shin I, Yakes FM, Rojo F, Shin N, Bakin AV, Baselga J and Arteaga CL. (2002). *Nat. Med.*, **8**, 1145–1152.
- Stenina OI, Poptic EJ and DiCorleto PE. (2000). *J. Clin. Invest.*, **106**, 579–587.
- Swamynathan SK, Varma BR, Weber KT and Guntaka RV. (2002). *Biochem. Biophys. Res. Commun.*, **296**, 451–457.
- Troussard AA, Mawji NM, Ong C, Mui A, St Arnaud R and Dedhar S. (2003). *J. Biol. Chem.*, **278**, 22374–22378.
- van Weeren PC, de Bruyn KM, de Vries-Smits AM, van Lint J and Burgering BM. (1998). *J. Biol. Chem.*, **273**, 13150–13156.
- Yahata H, Kobayashi H, Kamura T, Amada S, Hirakawa T, Kohno K, Kuwano M and Nakano H. (2002). *J. Cancer Res. Clin. Oncol.*, **128**, 621–626.
- Zhou BP, Liao Y, Xia W, Spohn B, Lee MH and Hung MC. (2001). *Nat. Cell Biol.*, **3**, E71–3.